

Textured $\text{Ca}_3\text{Co}_4\text{O}_9$ thermoelectric oxides by thermoforging process

M. Prevel, S. Lemonnier, Y. Klein, S. Hébert, and D. Chateigner

Cristallographie et Sciences des Matériaux (CRISMAT)—Ecole Nationale Supérieure d'Ingénieurs de Caen (ENSICAEN), Centre National de la Recherche Scientifique (CNRS)/Unité Mixte de Recherche (UMR) 6508, 6 Bd Maréchal Juin, 14050 Caen Cedex 4, France

B. Ouladdiaf

Institut Laue-Langevin (ILL), 6 rue J. Horowitz, BP 156-38042 Grenoble, Cedex 09, France

J. G. Noudem^{a)}

Cristallographie et Sciences des Matériaux (CRISMAT)—Ecole Nationale Supérieure d'Ingénieurs de Caen (ENSICAEN), Centre National de la Recherche Scientifique (CNRS)/Unité Mixte de Recherche (UMR) 6508, 6 Bd Maréchal Juin, 14050 Caen Cedex 4, France

(Received 8 June 2005; accepted 21 September 2005; published online 2 November 2005)

Using thermoforging process, dense $\text{Ca}_3\text{Co}_4\text{O}_9$ (Co349) thermoelectric oxides have been successfully textured. The various parameters influencing the formation of the Co349-textured material have been investigated. The electrical transport measurements show an anisotropy of the resistivity in good agreement with scanning electron microscopy observations. Texture is quantified by neutron-diffraction measurements and correlated to anisotropic resistivity measurements and Seebeck coefficients. © 2005 American Institute of Physics. [DOI: 10.1063/1.2120892]

INTRODUCTION

In contrast to the skutterudite compounds, there exists only few reports on processing and application of thermoelectric oxide materials. In spite of a limited effort, the misfit thermoelectric materials are now emerging as potential candidates for high-temperature devices. Some works have been devoted to the development of processing bulk thermoelectric oxides and the search for compounds^{1–6} with high figures of merit. Besides these oxides themselves, their preparation with satisfactory structural homogeneity, material density, and grain alignment are essential for the design of practical systems suitable for applications such as power generation. Especially, the optimization of platelet orientation is one of the main problems to overcome. Weak links at grain boundaries and low sample density, which affect the resistivity and consequently the figure of merit, are two reasons for improving the texturing technique.⁷ The figure of merit is defined as $ZT = S^2T/\rho\kappa$, with S being the Seebeck coefficient, T the temperature, ρ the electrical resistivity, and κ the thermal conductivity, and varies by six orders of magnitude^{5,8,9} in the literature. These differences are assumed to be related to the microstructures resulting from the use of different types of process: (i) conventional or spark plasma sintering,¹⁰ (ii) reactive templated grain growth,⁶ (iii) hot pressing,^{7,11} and (iv) magnetic texturation.¹²

In this paper, we report the results obtained on the polycrystalline $\text{Ca}_3\text{Co}_4\text{O}_9$ (Co349) thermoelectric oxide processed by thermoforging. This process allows to form the bulk textured materials having a good connection between the platelets in order to decrease the transport resistivity. The correlation between the microstructures and texture with the thermoelectric properties is investigated.

EXPERIMENT

The $\text{Ca}_3\text{Co}_4\text{O}_9$ powder was prepared by conventional solid-state reaction. Pure Co_3O_4 and CaCO_3 were mixed, calcined (900 °C, 12 h), and pressed uniaxially (30 MPa) into pellets. The samples were processed into the versatile setup using the thermomechanical schedule described in more detail elsewhere.¹³ Briefly, the pellet is heated at 920 °C for 24 h under various stresses (0–16 MPa) in air. For the microstructural analysis of the nonpressed and hot-forged samples, scanning electron microscopy (SEM) and energy dispersive x-ray spectroscopy (EDXS) were used. The chemical specimen composition after processing and the texture of the samples were investigated using x-ray diffraction (XRD) measurements on a Philips apparatus with $\text{Cu } K\alpha$ radiation and neutron diffraction using the D1B setup (Institut Laue-Langevin, Grenoble, France), respectively. Electrical resistivity was measured using a dc four-probe method using the Quantum Design PPMS system, a homemade high-temperature device, and a steady-state technique for Seebeck measurements, respectively. The measurements were performed in the temperature range from 5 to 700 K in self-field.

RESULTS AND DISCUSSION

Figure 1 shows cross-section SEM micrographs of the samples processed at 0, 7, and 16 MPa. The microstructure of the hot-pressed dense samples shows homogeneously distributed platelet-shaped ($>15 \mu\text{m}$) grains in contrast to the nonpressed sample where one can clearly observe some voids and platelet-shaped grains ($5 \mu\text{m}$). It can be seen that with increasing applied stress from 0 to 16 MPa, the grain size increased from 5 to $>15 \mu\text{m}$. Crystallite growth has been favored by hot forging as illustrated by the microstructures. In other words, crystallite growth is easier at larger stresses that improve grain contacts. These observations are

^{a)}Electronic mail: jacques.noudem@ensicaen.fr

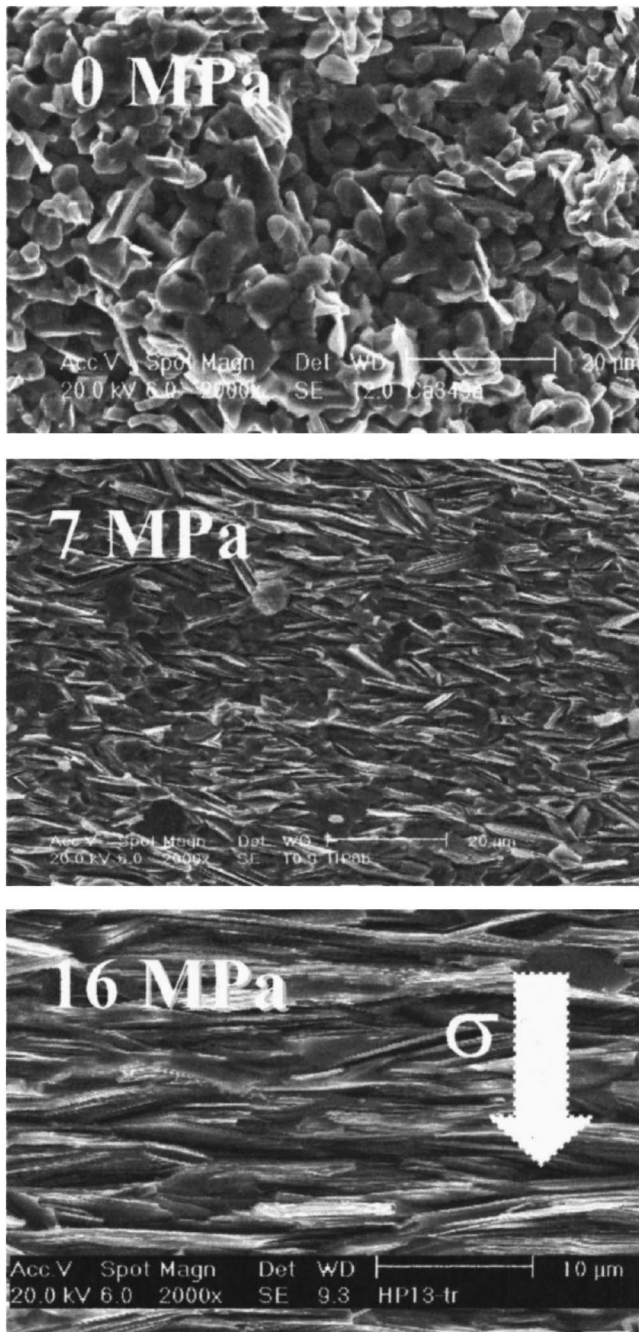


FIG. 1. SEM images of the cross section of the samples processed at various mechanical pressures.

correlated to the sample densities obtained from mass and volume determinations. The density increases from 3.10 g/cm^3 for the nonpressed sample to 4.65 g/cm^3 (with respect to the theoretical value of 4.92 g/cm^3) for the sample prepared at 16 MPa.

The temperature (T) dependence of the resistivity (ρ) for the reference $\text{Ca}_3\text{Co}_4\text{O}_9$ sample ($\sigma=0$ MPa) and the samples processed under 7 and 16 MPa, respectively, is shown in Fig. 2. For the thermoforged samples, the current was injected perpendicular to the processed stress direction; in this way the current flows essentially in the ab planes as seen in the high-magnification microstructure (Fig. 1, $\sigma=16$ MPa). The $\rho(T)$ curves show a similar behavior, corresponding to the

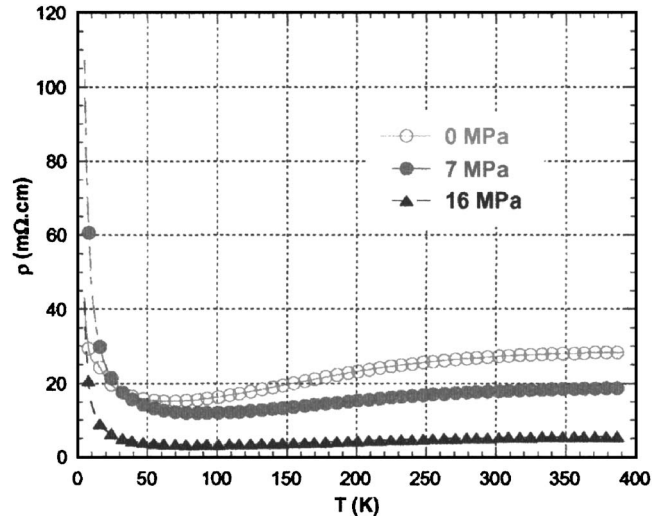


FIG. 2. Effect of synthesis stress (σ) on the room-temperature resistivity.

metal-to-semiconducting transition from high (400 K) to low temperature (5 K). This is in agreement with earlier reports^{2,5} on such thermoelectric oxides. These curves show that the room-temperature resistivity of the nonpressed sample is $27 \text{ m}\Omega \text{ cm}$ as compared to $18 \text{ m}\Omega \text{ cm}$ and not more than $5 \text{ m}\Omega \text{ cm}$ for the samples processed under 7 and 16 MPa, respectively. The decrease in resistivity values can be argued as due to the densification of the material under hot pressing and good alignment between platelets. The signature of the grain-boundary component on the resistivity seems to be low for the hot-forged samples. In addition, the resistivity (ρ) of the anisotropic sample is studied by using the Montgomery method.¹⁴ According to the sample geometry, the resistivity can be measured anisotropically by injecting the current and measuring the voltage between various configurations of the contacts [Fig. 3(a)]. Figure 3(b) shows the temperature dependence of the resistivity following the direction perpendicular and parallel to the stress applied during the thermoforging. From these measurements, we can clearly observe the transition around 50 K between the semiconducting behavior at low temperatures and the metallic state at high temperatures. One can also deduce an anisotropy ratio of 4 at room temperature, corresponding to the ratio of resistivities measured parallel (ρ^{\parallel} or ρ^{ab}) and perpendicular (ρ^{\perp} or ρ^c), respectively. It should be mentioned that the similar $\rho(T)$ behaviors have been obtained for the single crystals.² In that case the anisotropy ratio between out-of-plane (ρ^c) and in-plane (ρ^{ab}) resistivities was ~ 25 . The low anisotropy value obtained in our case seems to be related to the polycrystalline structure of the ceramic samples, where the weak links play an important role. The comparison with the sample processed without an applied stress using the same thermal conditions shows that, above room temperature, the resistivity value lies between the in-plane and out-of-plane configurations, but closer to the out-of-plane value, in agreement with the statistical random distribution of the crystallites.

The ρ value obtained for the nonforged sample is comparable to the values reported² on $\text{Ca}_3\text{Co}_4\text{O}_9$ prepared by conventional solid-state technique.

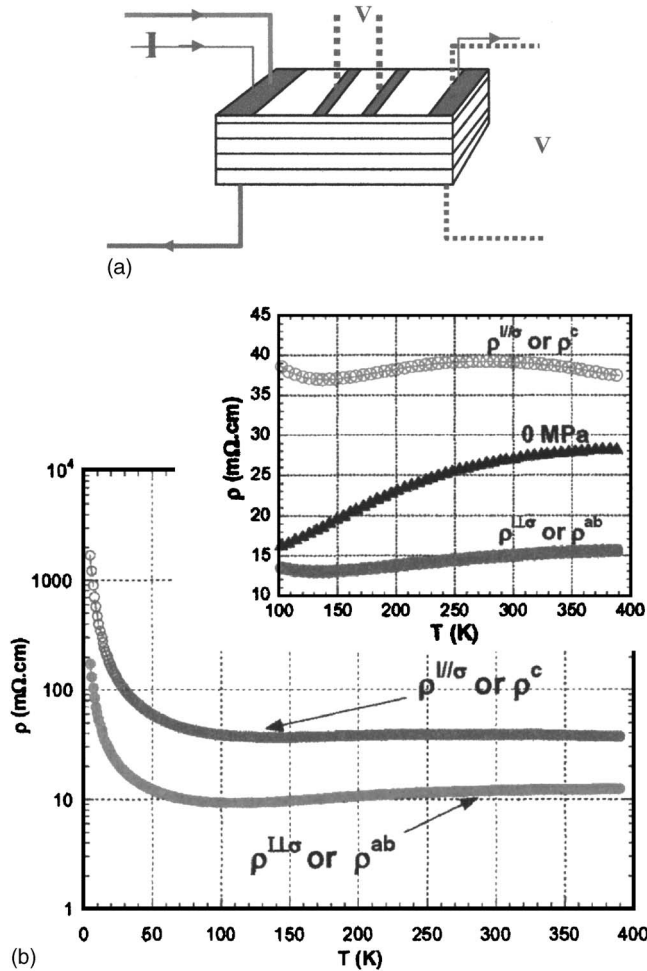


FIG. 3. (a) Sketch of the geometry used for measuring resistivity. (b) Temperature dependence of the resistivity ρ for current applied parallel (\circ) and perpendicular (\bullet) to the stress ($\sigma=7$ MPa) axis. (Inset) High magnification above room temperature showing the nontextured sample (\blacktriangle) between both configurations.

The temperature dependence of the Seebeck coefficient for the in-plane hot-forged ($\sigma=16$ MPa) samples is illustrated on Fig. 4. We can notice the positive values confirming the p -type conductor behavior. At room temperature the magnitude of $S=125 \mu\text{V/K}$ obtained can be compared with the data reported in the literature.^{5,6,12} The same sample has been measured at high temperatures (inset Fig. 4). The thermopower value above $120 \mu\text{V/K}$ is clearly confirmed.

Quantitative texture analysis of the anisotropic sample has been investigated using neutron-diffraction measurements. The texture data [Fig. 5(a)] show very strong intensity variations when the sample is tilted relative to the neutron beam. The combined analysis of the neutron data¹⁵ indicates that the $\{00\ell\}$ orientation is the unique component of texture as reported by Guilmeau *et al.*,⁷ with comparable texture strengths.

The texture is axially symmetric around the stress axis, giving rise to the $\{00\ell\}$ cyclic fiber texture. Figure 5(b) illustrates the achieved texture degrees at the intermediate (7 MPa) and largest applied pressure (16 MPa) using $\{004\}$ pole figures. The maximum orientation density on these fig-

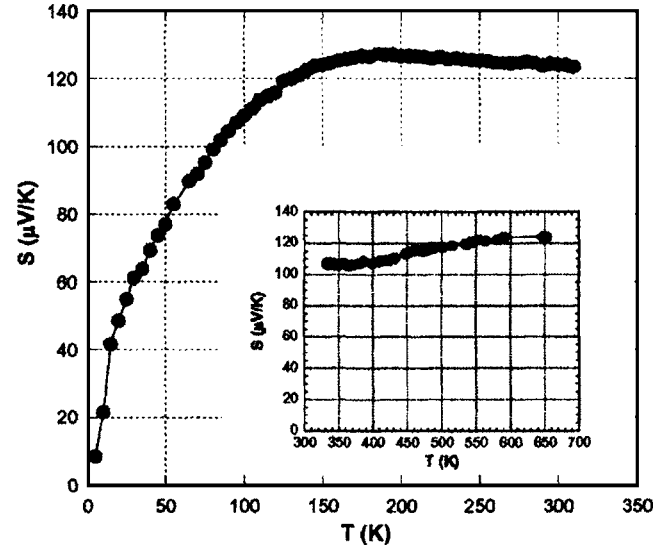


FIG. 4. Seebeck coefficient vs temperature for the hot-forged ($\sigma=16$ MPa) sample. Inset: Above room-temperature measurements.

ures are around 3.9 and 16.8 multiple of a random distribution (mrd) with 33% and 23% of the volume randomly oriented, respectively.

CONCLUSIONS

In summary, the thermoelectric oxide $\text{Ca}_3\text{Co}_4\text{O}_9$ bulks have been processed using a thermoforging technique. The pellets obtained are highly dense and strongly oriented with the mean c axis parallel to the stress direction applied during the heat treatment. Crystallite alignment of the bulk sample is confirmed by the strong texture as seen from the neutron-diffraction measurements and corresponds to the grain orientation as seen by the SEM measurements. The effect of thermomechanical processing is clearly evidenced by $\rho(T)$ curves. The resistivity decreases with increasing applied

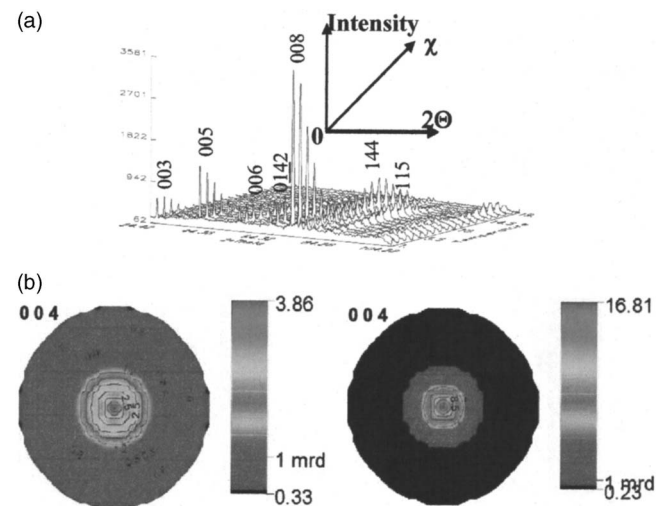


FIG. 5. (a) Neutron-diffraction diagrams measured at different tilt angles of the sample, which show the presence of a strong texture. (b) $\{004\}$ pole figures for the samples processed at 7 and 16 MPa (left and right, respectively) as extracted from Fig. 5(a) using the combined approach. The stress axis is perpendicular to the pole figure plane.

stress during heat treatment. This work shows that thermoforming allows one to produce samples with low resistivity in order to improve the figure of merit ZT.

ACKNOWLEDGMENTS

This work is supported by the Corning Company. One of the authors (M.P.) acknowledges a fellowship from the “French Ministère de la Recherche et de la Technologie.”

- ¹I. Terasaki, Y. Sasago, and K. Uchinokura, *Phys. Rev. B* **56**, R12685 (1997).
- ²A. C. Masset, C. Michel, A. Maignan, M. Hervieu, O. Toulemonde, F. Studer, and B. Raveau, *Phys. Rev. B* **62**, 166 (2000).
- ³M. Hervieu, A. Maignan, C. Michel, V. Hardy, N. Créon, and B. Raveau, *Phys. Rev. B* **67**, 045112 (2002).
- ⁴S. Hébert, S. Lambert, D. Pelloquin, and A. Maignan, *Phys. Rev. B* **64**, 172101 (2001).
- ⁵R. Funahashi, S. Urata, T. Sano, and M. Kitawaki, *J. Mater. Res.* **18**, 1646 (2003).
- ⁶T. Tani, H. Itahara, C. Xia, and J. Sugiyama, *J. Mater. Chem.* **13**, 1865 (2003).
- ⁷E. Guilmeau, R. Funahashi, M. Mikami, K. Chong, and D. Chateigner, *Appl. Phys. Lett.* **85**, 1490 (2004).
- ⁸W. Shin and N. Murayama, *Jpn. J. Appl. Phys., Part 2* **38**, L1336 (1999).
- ⁹G. Xu, R. Funahashi, M. Shikano, I. Matsubara, and Y. Zhou, *Appl. Phys. Lett.* **80**, 3760 (2002).
- ¹⁰I. Matsubara, R. Funahashi, T. Takeuchi, S. Sodeoka, T. Shimizu, and K. Ueno, *Appl. Phys. Lett.* **78**, 3627 (2001).
- ¹¹X. Gaojie, R. Funahashi, M. Shikano, I. Matsubara, and Z. Yugin, *J. Appl. Phys.* **91**, 4344 (2002).
- ¹²Y. Zhou *et al.*, *J. Appl. Phys.* **93**, 2653 (2003).
- ¹³V. Rouessac, J. Wang, J. Provost, and G. Desgardin, *Physica C* **268**, 225 (1996).
- ¹⁴H. C. Montgomery, *J. Appl. Phys.* **42**, 2971 (1971).
- ¹⁵D. Chateigner, *Combined Analysis: Structure-Texture-Microstructure-Phase-Stresses Determination by X-Ray and Neutron Diffraction*, <http://www.ensicaen.fr/~chateign/texture/combined.pdf>